Journal of Basic and Environmental Sciences, 5 (2018) 222-229

ISSN

Online: 2356-6388

Print: 2536-9202

Research paper

Open Access

Kinetic and thermodynamic studies on the removal of Cr (VI) ions from aqueous solution using n-ZVI

Eman. A. Kamar[1*], Hisham. M. Aly, Dalia. A. Amen

Department of chemistry, Faculty of Science, Benha University, Benha, Egypt, 13518

[1]*Corresponding author Email. Eman.kamar@fsc.bu.edu.eg

Abstract

We have studied the removal of Cr (VI) ion from aqueous solution at different condition using n-ZVI. The n-ZVI was prepared via borohydrate reduction under inert atmosphere. The effect of temperature, concentration and loading quantities on kinetic and equilibrium of chromium ion removal using n-ZVI were thoroughly examined. The prepared n-ZVI was characterized by several techniques including X-ray diffraction (XRD), transmission electron microscope (TEM) and scanning electron microscope (SEM). The adsorption capacity was found to be 40 mg g^{-1} at pH 3.9 and 300 K. The pseudo second order was found to be the best fitting kinetic model. The adsorption activation energy was calculated and given to be 41.56 kJ mol^{-1}. The thermodynamic parameters ΔG^o, ΔH^o and ΔS^o, were also calculated. The results indicate the endothermic and spontaneous nature of the adsorption process.

Keywords: Zero valent iron, Chromium, Thermodynamic, Kinetic, Nanoparticles.

Received; 5 May 2018, Revised form; 14 Jun 2018, Accepted; 14 Jun 2018, Available online 1 July. 2018

1. Introduction

In recent decades, the rapid increase in levels of environmental contamination has resulted in increasing concern for both human health and global ecosystems. Inorganic contaminants are heavy metals because of their toxicity towards aquatic-life, human beings, and the environment. Water pollution caused by heavy metal ions, such as Ni (II), Cr (VI), Mo (VI), and Pb (II) in ground water, is one of the most serious environmental problems. Among the toxic metal oxyanions, chromium is widely distributed and exists in the waste coming from paint industry, metal finishing, textile dyeing, electroplating, and leather tanning [1]. Chromium mainly exists as trivalent Cr (III) and hexavalent Cr (VI) form in the natural environment. Because of the low solubility, mobility, and the weak ability to oxidize other species, the toxicity of Cr (III) is much lower than Cr (VI) [2]. In contrast, Cr (VI) demonstrates the higher toxicity, which can produce mutagenic, teratogenicity, and carcinogenic effects in biological systems by reacting with nucleic acids and other cellular components [3]. Due to the high toxicity of Cr (VI), applying efficient methods to remove Cr (VI) from waste water is of great importance. So far, various kinds of methods have been developed to reduce the harmful effects of Cr (VI), such as chemical extraction [4], reduction-precipitation [5], ion exchange [6], bioleaching process [7, 8], and biosorption [9, 10].

Chemical precipitation may cause secondary pollution, and the electrolysis method is energy consuming and economically unfavorable. A large amount of high purity organic solvents is needed for liquid–liquid extraction and liquid membrane separation, most of which are harmful to the environment and health. Among these methods, adsorption holds the significant position due to its high removal efficiency, low energy demand, and less chemical investment [11-13]. In the past years, researchers have applied various adsorbents to remove Cr (VI) from waste water, such as activated carbons [14], zeolites [15, 16], clays [17], and non-magnetic particles [18]. However, these adsorbents have many defects including low porosity, low surface area, and lack of functional groups [19], which is of great importance for an efficient adsorbent. Hence, adsorbents with high porosity, large surface area, and high functionality need to be developed for efficient removal of Cr (VI). Alternatively, Nano scale zero-valent iron (n-ZVI) has shown good potential to remove metal ions and other aqueous organic pollutants. Such as, its physicochemical properties and reductive capacity can facilitate rapid decontamination of polluted water and the removal rate is extremely high [20, 21]. Limited numbers of publications have been reported to illustrate the thermodynamics and activation energy calculations of the chromium ion adsorption using nZVI adsorbate [22, 23].

In this study, we have investigated the kinetic and adsorption isotherm models for chromium ion removal using nZVI. Different thermodynamic parameters and activation adsorption energy were calculated. Furthermore, the core shell model was verified manipulating the obtained results.

2. Materials and methods

All chemicals were of analytical grades and used as received. Deoxygenated deionized water (DDI) was used in the preparation of reagent solutions. However, the nitrogen atmosphere was maintained throughout the experiment process. $FeCl_3.6H_2O$, $NaBH_4$, NaOH pellets, HCl, $K_2Cr_2O_7$ and dehydrated ethanol were supplied by

Sigma Aldrich. DDI water was prepared by passing pure nitrogen gas through DI water at a flow rate 100 ml per minute for 2 hours.

2.1. Preparation of n-ZVI

The black solids n-ZVI was prepared as previously reported [21]. Briefly, in 3 neck flask, 50 ml (0.02M) of $NaBH_4$ was added to 50 ml of (0.05M) $FeCl_3.6H_2O$ dropwise, while the mixture was vigorously stirred by the aid of mechanical stirring at 400 RPM at room temperature. The n-ZVI was collected and washed with DDI water, followed by the dehydrated absolute ethanol. The prepared n-ZVI was dried under vacuum at room temperature in nitrogen atmosphere. Finally, it was stored in a vacuum desiccator.

2.2 Characterization

The surface morphology of n-ZVI was studied using field emission electron microscope (FE-SEM, JEOI6390) and high resolution electron microscope (HR-TEM, JEM2100).

2.3 Kinetic studies

Kinetic studies of Cr (VI) removal from aqueous solutions were carried out in different conditions of Cr (VI) concentration, loading amount of n-NZVI and at different temperatures.

Preliminary experiments were carried out to study the effect of pH. The results showed that the maximum removal is obtained at pH 3.9. Accordingly, all further experiments were carried out at pH 3.9. The loading effects of n-ZVI on the Cr (VI) kinetic removal were investigated using 0.03, 0.05 and 0.07 g added to 20 ml of Cr (VI) solution. The effect of different concentrations was studied using 75, 100, 150 and 200 ppm of Cr (VI). Samples were collected at different time intervals for Cr (VI) analysis. The adsorped Cr (VI) concentration was measured using UV–Visible spectrophotometer, Jasco model V670. Adsorption isotherms were carried out at different Cr (VI) initial concentration 75,100,150 and 200 ppm and temperatures of 27,30 and 40 C°. The samples were collected after equilibrium time and analyzed for Cr (VI) concentration.

The amount of Cr (VI) removal was estimated using the following equation,

$$q_e = C_o - C_t \times \frac{V}{m} \qquad (1)$$

Where; C_o and C_t is the initial and the concentration at time t, V is the volume of the solution (ml) and m is the mass of the solid n-ZVI (g).

2.4 Kinetic models

Different kinetic models are used to examine the experimental results of Cr (VI) removal. Pseudo first order, pseudo second order, and intraparticle diffusion models are utilized to reveal the adsorption kinetics process. The linear form of these models can be expressed as,

Pseudo first order

$$\ln (q_e - q_t) = \mathrm{Ln} q_e - K_1 t \qquad (2)$$

Pseudo second order

$$\frac{t}{q_t} = \frac{1}{K_2 q_e^2} + \frac{t}{q_e} \qquad (3)$$

Intraparticle diffusion

$$q_e = K_p t^{0.5} + I \qquad (4)$$

Where q_e and q_t (mg g^{-1}) the adsorption capacities at equilibrium and at time t (min). K_1 (min^{-1}) and K_2 (g mg^{-1} min^{-1}) are the rate constant of pseudo first order and second order, respectively. K_P (mg g^{-1} $min^{0.5}$) is the intraparticle diffusion rate constant and I is the intercept.

2.5 Adsorption activation energy

Adsorption activation energy was calculated using Arrhenius equation (5) extracted from the pseudo second order model; the most fitted kinetic models. The plot of ln K_2 against inverse temperature yields a straight line with slope –Ea/R

$$K_2 = K e^{\frac{-E_a}{R}} \qquad (5)$$

Where: K is the temperature independent constant (g mg^{-1} min^{-1}), E_a sorption activation energy (KJ mol^{-1}), R the universal gas constant (8.312 J mol^{-1} K) and T the absolute solution temperature.

2.6 Adsorption isotherm models

2.6.1 Langmuir isotherm

This type of isotherm postulate the adsorption occurred in a monolayer adsorption on a regular surface with confined a sorption sites. The linear equation of Langmuir isotherm is given by,

$$\frac{C_e}{q_e} = \frac{C_e}{q_m} + \frac{1}{K_L q_m} \qquad (6)$$

Where q_m is the maximum adsorption capacity (mg g^{-1}) and K_L is the Langmuir constant relate to the adsorption energy [24].

2.6.2 Freundlich isotherm

The Freundlich isotherm assumes monolayer and multilayer adsorption onto heterogeneous surface of an adsorbent [24]. The form of Freundlich equation is given by,

$$\ln q_e = \ln K_F + \frac{1}{n} \ln C_e \qquad (7)$$

Where K_F and n are isotherm constants related to adsorption capacity and adsorption intensity, respectively, and C_e is the equilibrium concentration (mg L^{-1}) [24].

2.6.3 Temkin isotherm

The linear form of Temkin isotherm is expressed as:

$$q_e = \frac{R}{b} \ln K_T + \frac{R}{b} \ln C_e \qquad (8)$$

Where b is the Temkin constant related to the heat of sorption (J mol^{-1}) and K_T is the Temkin isotherm constant (L g^{-1}) [24].

2.6.4 The thermodynamic parameters

The thermodynamic equilibrium constant K_a was used to calculate the thermodynamic parameters. K_a is given by,

$$K_a = \frac{a_s}{a_e} = \frac{\gamma_s}{\gamma_e} \frac{C_s}{C_e} \qquad (9)$$

Where a_s the activity of the adsorbed ion, a_e the activity in solation at equilibrium, γ_s and γ_e are the corresponding activity coefficient. However, C_s is the Cr (VI) adsorbed on n-ZVI (m mol g^{-1}), and C_e is the concentration in equilibrium solution (m mol mL^{-1}).

However, ΔG^O (standard Gibbes free energy KJ mol^{-1}), ΔH^O (standard enthalpy change KJ mol^{-1}) and ΔS^O (standard entropy change J mol^{-1} K^{-1}) were calculated using the standard Gibbes free energy equation (10),

$$\Delta G^o = -RT \ln K_o \qquad (10)$$

K_O was obtained from the slop of a linear plot of $\ln \frac{C_s}{C_e}$ against C_s. The slope of ln K_O at different temperature

against $\frac{1}{T}$ allows calculating the standard thermodynamic parameters.

3. Results and Discussion

3.1 Characterization of n-ZVI

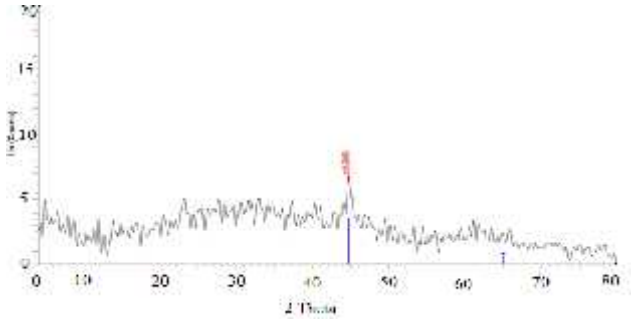

Fig (1): XRD patterns of the prepared n-ZVI.

The TEM analysis showing in fig (2a) revealing the formation of nanoparticles with particle size distribution between 15-25 nm. However, it is clear that limited agglomerate has been occurred. Surface morphology was characterized by SEM as shown in figure (2b). The SEM image shows dendritic structure. This can be attributed to the formation of an envelope of iron oxide and iron hydroxide according to the inner core structure of n-ZVI [26]. The SEM image shows a cave like structure due to the formation condition which controls the evolution of each n-ZVI particle [27].

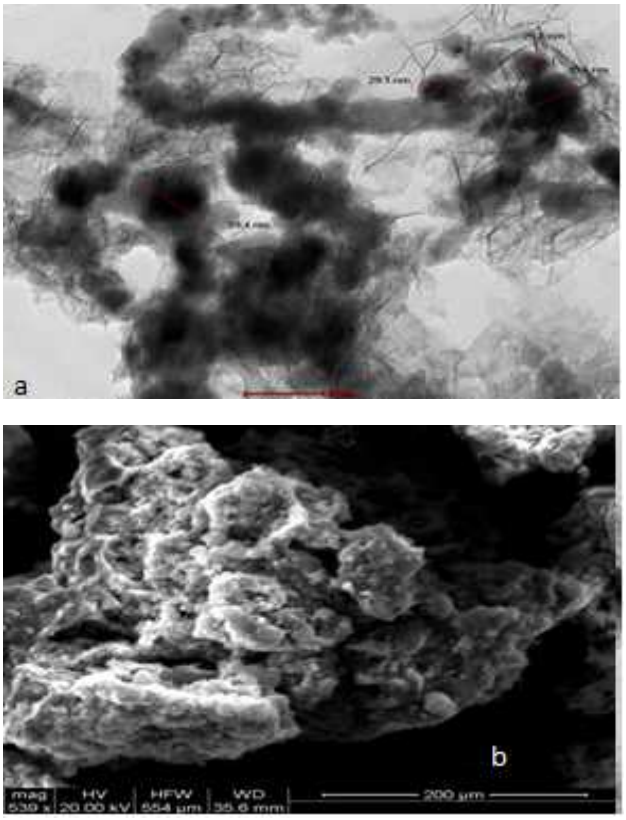

Fig (2): TEM (a) and SEM (b) images for the synthesized nZVI particles

Figure (1) shows the XRD patterns of the prepared n-ZVI. It reveals the peak of zero valent iron at 44.76° in agreement with ASTM carb number 88-2324 [25], indicating the face centered cubic lattice structure.

3.2 Adsorption kinetics

Different parameters of adsorbent loading, Cr VI) concentrations, and temperature, were investigated. The figures 3-5 show the equilibrium is attained after 3.5 hours.

Pseudo first order, pseudo second order and intraparticle diffusion models have been used to evaluate the kinetic of the adsorption process.

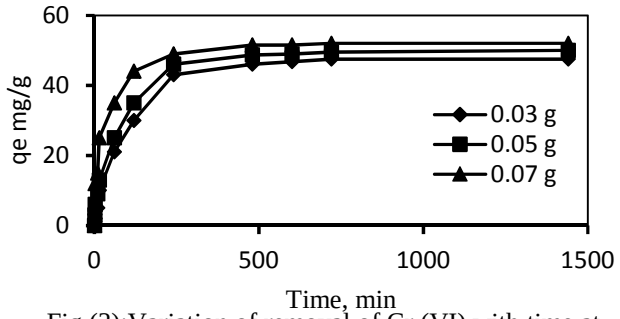

Fig (3):Variation of removal of Cr (VI) with time at different loading adsorbent

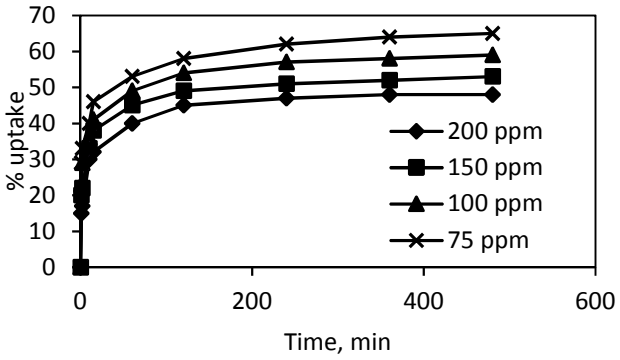

Fig (4): Effect of Cr VI concentration on the sorption kinetics by nZVI at 300 K and pH 3.9.

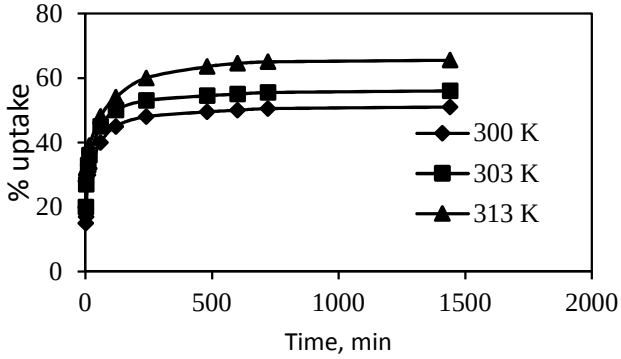

Fig (5): Effect of temperature on the % uptake of Cr(VI) using 0.05 g nZVI at different temperature and pH 3.9.

3.2.1 Pseudo first order

The slope and intercept of linear plots of ln (q_e-q_t) verse t were used to calculate the velocity (K_1) and the sorption capacity at equilibrium, as shown in figure (6) and table (1). According to the law value of R^2 the pseudo first order is not adequate to interpret the adsorption of Cr (VI) on n-ZVI [28].

3.2.2 Pseudo second order

The parameters of the pseudo second order were tabulated and given in table (1). The high linearity fitting R^2 obtained from the t/qe versus t plot figure (7) indicates the proper application of the pseudo second order to illustrate the adsorption kinetic of Cr (VI) using n-ZVI. Both values of K_2 and initial velocity indicate that the adsorption process has a chemical interaction. Similar manner has been reported for the adsorption using n-ZVI Figure (8, 9) [28].

Table (1): Kinetic parameters of pseudo first and pseudo second-order models of Cr (VI) removal using nZVI at pH 3.9 and 300 K.

Parameters	Different loading at Cr (VI) 200 ppm			Different cons. (ppm) at 0.05 loading		
n-ZVI	0.03	0.05	0.07	75	100	150
Pseudo first-order						
qe (mg g^{-1})	32.61	17.4	14.35	8.51	9.72	14.33
k1 x103 (min^{-1})	5.6	5.6	5.3	4.2	3.9	5.6
R^2	0.95	0.87	0.862	0.857	0.843	0.754
Pseudo second-order						
qe (mg g^{-1})	58.14	38.61	31.75	19.61	23.75	31.94
k2x103 (min^{-1})	1.25	3.31	3.83	6.81	6.13	4.82
h (mg $g^{-1}min^{-1}$)	4.23	4.93	3.89	2.62	3.45	4.92
R^2	0.986	0.989	0.978	0.932	0.881	0.896

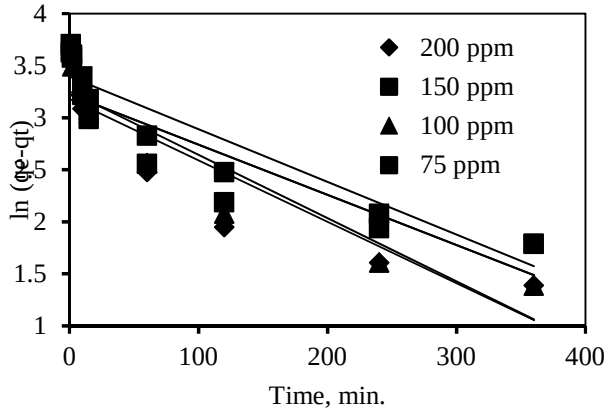

Fig (6): Pseudo first order Plots of different Cr(IV) ion concentrations at 0.05 g nZVI adsobent and 300 K.

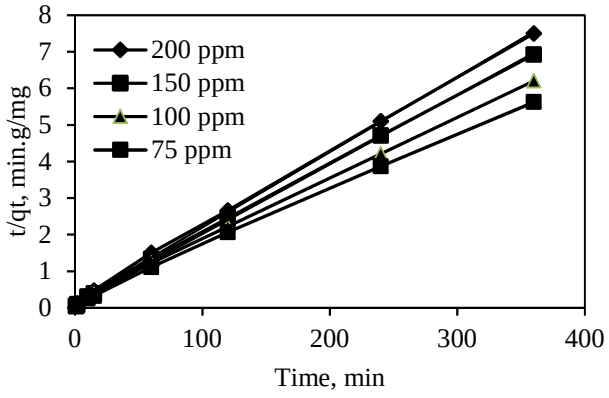

Fig (7): Pseudo second order Plots of different Cr(IV) ion concentrations at 0.05 g loading nZVI adsobent and 300K.

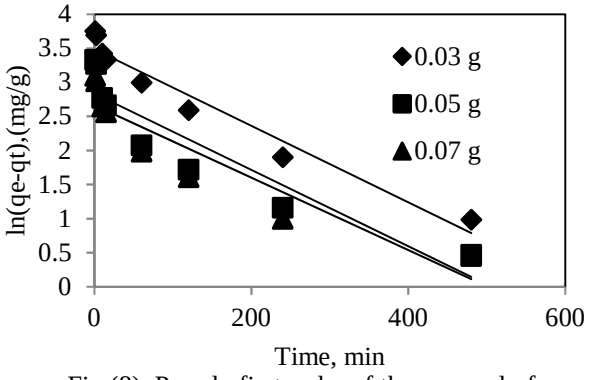

Fig (8): Pseudo first order of the removal of Cr(VI) with different loading adsorbent of nZVI.

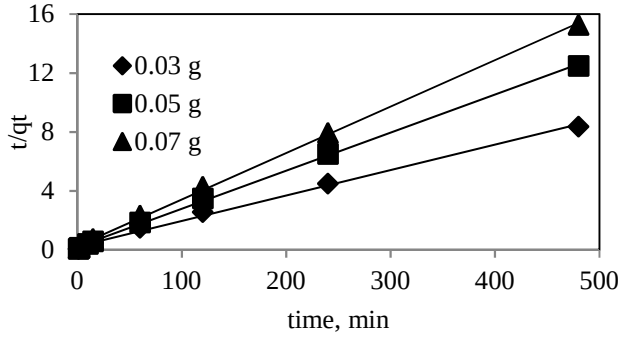

Fig (9): Pseudo second order of the removal of 200 ppm Cr(VI) ion with different loading absorbent on nZVI at 300 K.

3.2.3 Intraparticle diffusion model

The adsorption process can be optimized through understanding the adsorption mechanisms to reveal the rate determine step. It can be accomplished through definite steps [24]: (1) film adsorption to the sorbent particles, (2) sorbet diffusion to the core of the sorbent.

Finally, adsorption to specific site by chemical or physical attraction.

The plot of q_t verses $t^{0.5}$ figures (11, 12) show two steps. This proposes that the adsorption takes place in two steps. The first step is the faster one represents the film formation and the second step is the reduction step of Cr (VI) ion. The plots did not pass across the origin indicating that the intraparticle diffusion is not the rate determine step, although it may take place in the adsorption process.

K_1which represent the film formation rate constant is much faster than that of the equilibrium rates shown in table (2). However, the C term, the value of the intercept, is related to the thickness of different step.

The values of C_1 and C_2 calculated from the first and second steps disclose the thickness of the film formed on the surface of the n-ZVI is much less than the inner boundary layer. These results support the proposed core shell model of the n-ZVI.

Table 2. The kinetic parameters of intraparticle diffusion of Cr (VI) removal using n-ZVI at pH 3.9 and 300 K.

Parameters	Different loading at Cr (VI) 200 ppm			Different cons. (ppm) at 0.05 loading		
	0.03	0.05	0.07	75	100	150
n-ZVI						
K_1 (mg $g^{-1}min^{-1}$)	5.15	5.04	3.27	1.62	2.25	3.77
C_1 (mg g^{-1})	12.5	6.88	7.84	7.27	7.59	8.04
R^2	0.996	0.985	0.987	0.976	0.959	0.998
K_2 (mg $g^{-1}min^{-1}$)	1.53	0.563	0.507	0.245	0.266	0.316
C_2 (mg g^{-1})	28.99	27.92	2.212	14.4	18.17	25.27
R^2	0.986	0.989	0.978	0.932	0.881	0.896

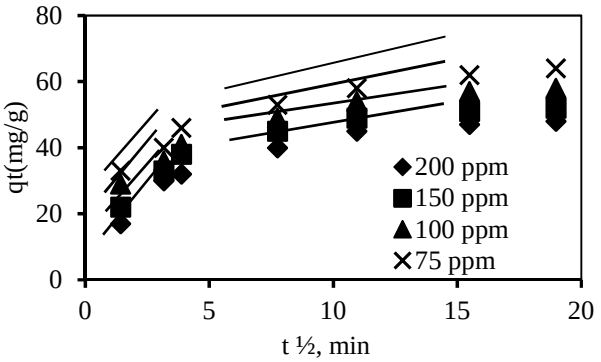

Fig (10): Intraparticle diffusion Plots of different Cr(IV) ion concentrations at 0.05 g loading nZVI adsobent and 300K.

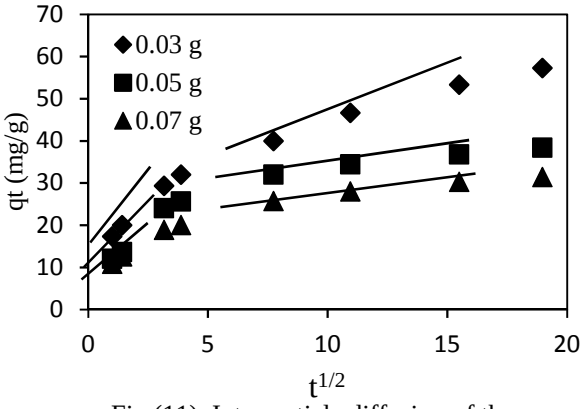

Fig (11): Intraparticle diffusion of the removal of Cr (IV) with different loading adsorbent of nZVI.

3.3 Activation energy of the adsorption

Figure 12, shows the plot of $\ln K_2$ against 1/T. The adsorption activation energy (E_a) was calculated from the slope and given to be 41.56 KJ mol^{-1}. The calculated value of the activation energy is more than 40 KJ mol^{-1} indicating the nature of chemical adsorption of Cr (VI) using nZVI.

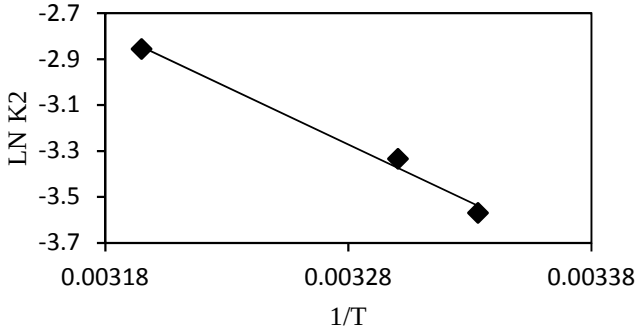

Fig (12): Plot of Ln Kl versus 1/T for Cr(VI) adsorption on nZVI at pH 3.9

3.4 Adsorption Isotherms

Different adsorption isotherms models Langmuir, Freundlich and Temkin were tested to analyze the adsorption of Cr (VI) ions by n-ZVI.

3.4.1 Langmuir Isotherm

The calculated Langmuir parameters q_m and K_L were obtained from the slope and intercept of C_e/q_e versus C_e figure (13) at different temperature and given in table (3). The R^2 are 0.99 at room temperature and decrease with increasing temperature to give 0.92 at 313 K.

The Cr (VI) adsorption capacity on n-ZVI increase with increasing temperature. The calculated adsorption capacity is higher than that reported earlier [24].

3.4.2 Freundlich Isotherm

The different parameters of Freundlich isotherm were calculated and given at table (3). The K_f and n parameters are calculated from the intercept and slope of the linear plot of $\ln q_e$ against $\ln C_e$, as shown in figure (14). The values of n, is more than unity representing the L-type isotherm characteristic of chemisorption adsorption type [24].

The values of K_f show an increase with increasing temperature reflect action of endothermic adsorption process.

3.4.3 Temkin Isotherm

The plot of Temkin adsorption isotherm figure (15) shows linearity at all the different temperatures studied.

The will fitting correlation linearity of value of 0.99 as shown in table (3) supporting the conclusion of an endothermic process of adsorption**.**

Table (3): Isotherm models parameters for adsorption of Cr (IV) by n-ZVI particles at different temperature.

Isotherm	Temperature	Parameters		
		n-ZVI		
Freundlich		K_f	n	R^2
	300	1	1	1
	303	05.57	1.93	0.999
	313	10.06	2.55	0.980
Langmuir		qm	K_L	R^2
	300	64.10	5.50E-2	0.992
	303	65.79	3.56E-2	0.981
	313	67.11	2.85E-2	0.924
Temkin		K_T	b	R^2
	300	0.243	167.06	0.991
	303	0.330	170.89	0.989
	313	0.773	203.61	0.959

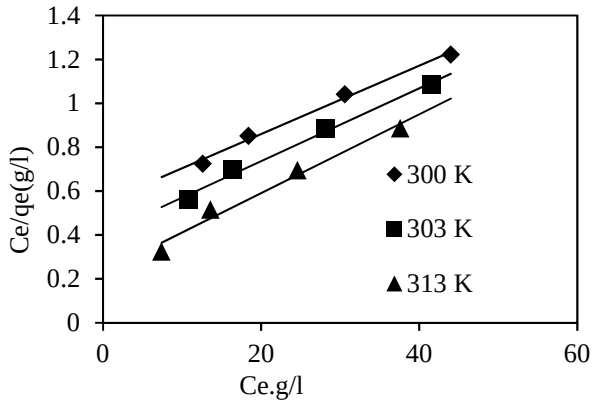

Fig (13): Langmuir isotherm model for Cr (VI) adsorbtion by n-ZVI at different temperature

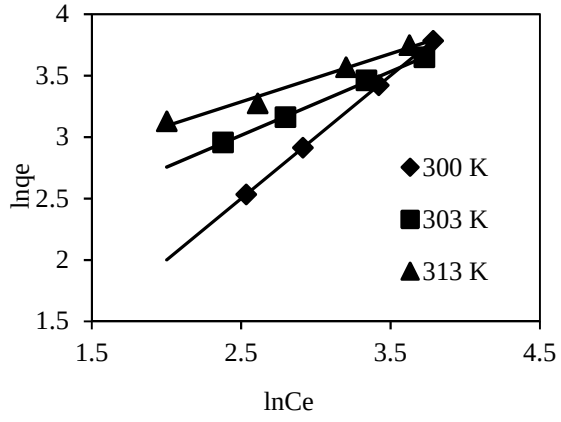

Fig (14): Freundlich isotherm model for Cr (VI) adsorbtion by n-ZVI at different temperature

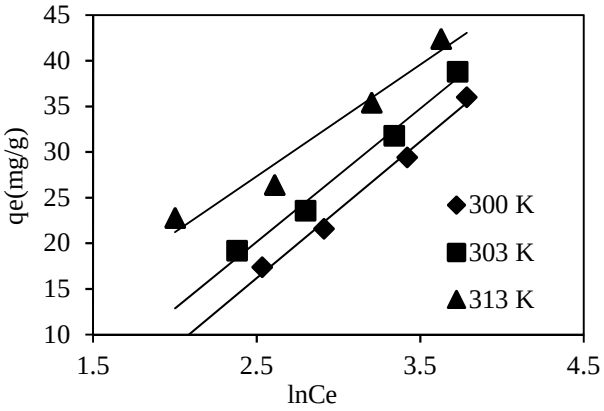

Fig (15): Temkin isotherm model for Cr (VI) adsorbtion by n-ZVI at different temperature

4. Thermodynamic studies

The thermodynamic equilibrium constant K_o at different temperature was estimated from the linear plots of ln (C_s/C_e) against C_s as shown in figure (16). As the temperature increased the K_o increased supporting the endothermic adsorption as indicated from the isotherm studies. The standard thermodynamic parameters were calculated and given in table (4). ΔG^0 show negative values indicating spontaneous adsorption process. The ΔH^0 and ΔS^0 were evaluated from the plot of $\ln K_o$ versus 1/T as shown in figure (17). The positive ΔH^0 values confirm the endothermic nature of Cr (VI) toward the n-ZVI nanoparticles. However, the affinity of n-ZVI for Cr (VI) was reflected through the positive value of the standard entropy [24].

Table (4): Thermodynamic parameters for Cr (VI) adsorption onto n-ZVI.

Temperature (K)	K_o	ΔG^o KJmol^{-1}	ΔH^o KJ mol^{-1}	ΔS^o mol^{-1}K^{-1}
300	1.50	-1.01		
303	1.86	-1.54	24.45	85.31
313	2.33	-2.11		

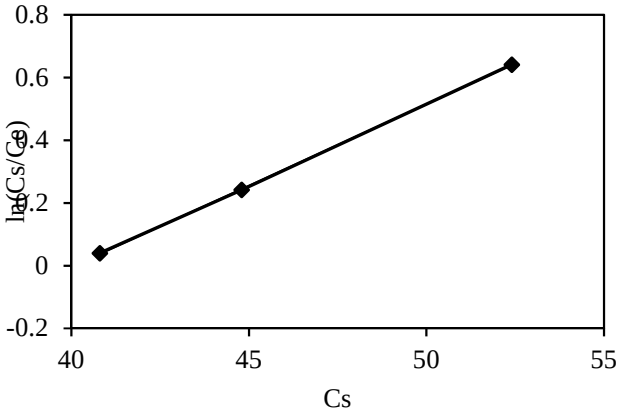

Fig (16):. A plot of ln (Cs/Ce) versus Cs at various temperature of nVZVI .

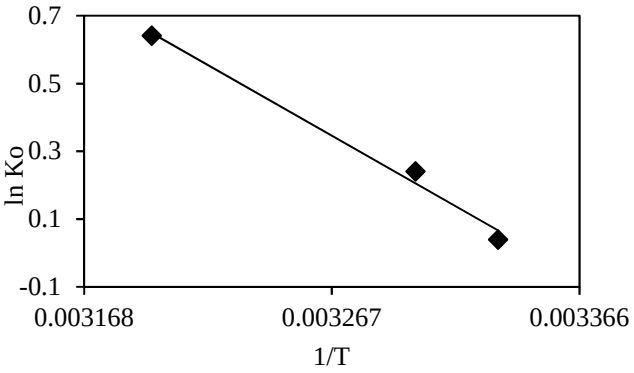

Fig (17): A plot of ln Ko versus 1/T at various temperature of nVZVI.

5. Summary and conclusion

In this study, the kinetics of adsorption of Cr (IV) using n-ZVI has been investigated by pseudo first and second order models. Also, the intraparticle diffusion model was tested. The calculations indicated that the pseudo second order is the most fitted model among the other models with high R^2 value. The adsorption isotherm was tested applying Langmuir, Freundlich and Temkin models. The Freundlich isotherm showed a best fit isotherm indicating the multilayer adsorption of Cr (VI) toward the n-ZVI surface. The kinetic and thermodynamic calculations and the adsorption activation energy proven that the overall adsorption process was spontaneous and endothermic in nature.

Reference

[1] S.Avudainayagam, M.Megharaj, G.Owens, R.S.Kookana, D. Chittleborough, R. Naidu, Chemistry of chromium in soils with emphasis tannery waste sites, Reviews of Environmental Contamination and Toxicology. 178 (2003) 53-91.

[2] L. Zhang, W. Xia, X. Liu, W. Zhang, Synthesis of titanium cross-linked chitosan composite for efficient adsorption and detoxification of hexavalent chromium from water, Journal of Materials Chemistry A. 3 (2014) 331- 340.

[3] Y. Ishibashi, C. Cervantes, S. Silver, Chromium reduction in Pseudomonas putida, Applied and Environmental Microbiology. 56 (1990) 2268-2270.

[4] P. J. C. Favas, J. Pratas, M. E. P. Gomes, V. Cala, Selective chemical extraction of heavy metals in tailings and soils contaminated by mining activity: Environmental implications, Journal of Geochemical Exploration. 111 (2011) 160-171.

[5] E. Sahinkaya, A. Kilic, Heterotrophic and elemental-sulfur based autotrophic denitrification processes for simultaneous nitrate and Cr (VI) reduction, Water Research. 50 (2014) 278-286.

[6] J. H. Chen, K. C. Hsu, Y. M. Chang, Surface modification of hydrophobic resin with tricaprylmethy ammonium chloride for the removal of trace hexavalent chromium, Industrial and Engineering Chemistry Research. 52 (2013) 11685-11694.

[7] H. Ma, J. Zhou, L. Hua, F. Cheng, L. Zhou, X. Qiao, Chromium recovery from tannery sludge by bioleaching and its reuse in tanning process, Journal of Cleaner Production. 142 (2017) 2752- 2760.

[8] M.Qu, J. Chen, Q. Huangetal, Bioremediation of hexavalent chromium contaminated soil by a bioleaching system with weak magnetic fields, International Biodeterio ration & Biodegradation. (2016) .

[9] S. Nag, A. Mondal, N. Bar, S. K. Das, Biosorption of chromium (VI) from aqueous solutions and ANN modelling, Environmental Science and Pollution Research. 24 (2017) 1-9.

[10] J. Zhao, X. Zhang, X. He, M. Xiao, W. Zhang, C. Lu, A super biosorbent from dendrimer poly (amidoamine) -grafted cellulose nanofibril aerogels for effective removal of Cr (VI), Journal of Materials Chemistry A. 3 (2015) 14703-14711.

[11] Y. J. Jiang, X. Y. Yu, T. Luo, Y. Jia, J. H. Liu, X. J. Huang, Fe_2O_3 nanoparticles encapsulated millimeter-sized magnetic chitosan beads for removal of Cr (VI) from water: Thermodynamics, kinetics, regeneration, and uptake mechanisms, Journal of Chemical and Engineering Data. 58 (2013) 3142-3149.

[12] Y. Liu, C. Luo, G. Cui, and S. Yan, Synthesis of manganese dioxide/iron oxide/graphene oxide magnetic nanocomposites for hexavalent chromium removal, RSC Advances. 5 (2015) 54156-54164.

[13] B. Qiu, H. GU, X. Yan et al., Cellulose derived magnetic mesoporous carbon nanocomposites with

enhanced hexavalent chromium removal, Journal of Materials Chemistry A. 2 (2014) 17454-17462 .
[14] H. Liu, S. Liang, J. Gaoetal., Enhancemen of Cr (VI) removal by modifying activated carbon developed from Zizaniacaduciflora with tartaric acid during phosphoric acid activation, Chemical Engineering Journal. 246 (2014) 168-174.
[15] R. V. Kumar, A. K. Basumatary, A. K. Ghoshal, and G. Pugazhenthi, Performance assessment fananalcime-C zeolite ceramic, composite membrane by removal of Cr (VI) from aqueous solution, RSC Advances. 5 (2015) 6246-6254.
[16] W. X Wang, Y. Qiao, T. Lietal., Improved removal of Cr (VI) from aqueous solution using zeolite synthesized from coal fly ash via mechano-chemical treatment, Asia-Pacific Journal of Chemical Engineering. 12 (2017) 259-267.
[17] L. Deng, Z. Shi, B. Li, L. F. Yang, L. Luo, X. Z. Yang, Adsorption of Cr (VI) and phosphate on Mg-Al hydrotalcite supported kaolin clay prepared by ultrasound-assisted coprecipitation method using batch and fixed-bed systems, Industrial & Engineering Chemistry Research. 53 (2014) 7746-7757.
[18] W.B. Zhang, M. Deng, C. X. Sun, S.B. Wang, Ultrasound-enhanced absorption of chromium (VI) on Fe_3O_4 magnetic particles, Industrial and Engineering Chemistry Research. 53 (2014) 333-339.
[19] B. Sarkar, Y. Xi, M. Megharaj, G. S. R. Krishnamurti, D. Rajarathnam, R. Naidu, Remediation of hexavalent chromium through adsorption by bentonite based arcade 2HT-75 organoclays, Journal of Hazardous Materials. 183 (2010) 87-97.
[20] X. Li, D. W. Elliott, W. Zhang, Zero-valent iron nanoparticles for abatement of environmental pollutants: materials and engineering aspects, Crit. Rev. Solid State Mat. Sci. 31 (2006) 111-122 .
[21] Y.P. Sun, X.Q. Li, J. Cao, W.X. Zhang, H.P. Wang, Characterization of zero-valent iron nanoparticles, Adv. Colloid Interface Sci. 120 (2006) 47-56.
[22] M. Arshadi, M. Soleymanzadeh, J.W.L. Salvacion, F. S.Vahid, Nanoscale Zero-Valent Iron (NZVI) supported on sineguelas waste for Pb (II) removal from aqueous solution: Kinetics, thermodynamic and mechanism, Journal of Colloid and Interface Science. 426 (2014) 241-251.
[23] A. K. Hameed, N. Dewayanto, D. Dongyun, M. R. Nordin, M.H.Ab. Rahim, Kinetic and Thermodynamics of Methylene Blue Adsorption onto Zero Valent Iron Supported on Mesoporous Silica, Bulletin of Chemical Reaction Engineering & Catalysis. 11 (2) (2016) 250-261.
[24] H.K. Boparai, M. Joseph, D. M. O. Carroll, Kinetics and thermodynamics of cadmium ion removal by adsorption onto nano zerovalent iron particles, Journal of Hazardous Materials. 185 (2011) 458-465.
[25] J. Hàglund, A. Fernaedz, G. Grimvall, M. Kòrling, Theory of bonding in transition metal carbides and nitrides, American Phys. Soci. Rev. B. 48 (1993) 115-116 .
[26] Z. Fang, X. Qiu, X. Huang, M.Li, Removal of chromium in electroplating wastewater by nanoscale zero –valent metal with synergistic effect of reduction and immobilization, Disalination. 280 (2011) 224-231.
[27] Z. Yale, C. Wen, D. Chaomeng, Z. Chuanlong, Z. Xuefei, Structural evolution of nanoscale zero valent iron (n-ZVI) in a noxic Co^{2+} solution: Interactional performance and mechanism, Scientific report. 5 (2015) 13966-13975.
[28] Y. C. Sharma, V. Srivastava, C. H. Weng, S. N. Upadhyay. Removal of Cr (VI) From Wastewater by Adsorption on Iron Nanoparticles, The Canadian journal of chemical engineering. 87 (2009) 921-929.